2020 IEEE/RSJ International Conference on Intelligent Robots and Systems (IROS)
October 25-29, 2020, Las Vegas, NV, USA (Virtual)

Automated Design and Construction of a Single Incision Laparoscopic System Adapted to the Required Workspace

Sandra V. Brecht, Johannes S. A. Voegerl, and Tim C. Lueth, *Member, IEEE*

***Abstract*— Currently, laparoscopic surgery systems are adapted for a large number of indications and patients and are therefore not optimized for one specific case.**

The challenge to create systems with an optimized kinematic structure for a specific patient regarding reachability and manipulability in the needed workspace is the automated design and construction process.

We have developed an automated design and construction process for a patient-specific Single Incision Laparoscopic System that is optimized for a specific indication, procedure, patient, and surgeon. The kinematic structure is adapted to the required workspace, needed instrumentation, and manufacturing parameters.

First results show that the patient-specific Single Incision Laparoscopic System is better suited for the specific application regarding the combination of reachability, manipulability, and system size in the required workspace than the standard Single Incision Laparoscopic System in different standard sizes or one simple standard size.

I. INTRODUCTION

Currently, a trend exists for an individualized treatment of different patients with patient-specific medical products to achieve the best outcome for every individual patient.

Patient-specific medical products such as implants or surgical guides and templates are predominantly adapted to the patient's anatomy by using preoperative imaging to determine the input parameters for the design, a parameterized design and construction process, and 3D printing as the manufacturing technology [1].

In single incision laparoscopic surgery, the indication for the procedure and the patient's anatomy are crucial for the selection of an appropriate procedure and the instrumentation for the treatment. The workspace needed for the procedure is an especially relevant factor. The aim is to have a high reachability with the selected instrumentation in this workspace, which means that it can reach as many positions as possible in at least one orientation. Furthermore, the instrumentation has to have high manipulability in order to reach the positions in as many orientations as possible [2]. For single incision laparoscopic systems with a shaft and arms that are opened inside the body (Y type systems), the reachable workspace depends on the kinematic structure of the arms [3].

Additionally, the needed forces should be available at the effector's tip for tissue manipulation and the accuracy at the effector's tip should be high [3]. Therefore, for type Y single incision systems, the ratio of the forces at the effector's tip to the arm length is relevant. Longer arms need higher actuation forces and have higher flexibility, which results in a higher displacement of the effector's tip and therefore lower accuracy. Systems with shorter arms are therefore preferred, but at the same time it must be assured that a high reachability and manipulability in the needed workspace is achieved with the kinematic structure of the deployed arms.

The adaptation of a kinematic system to the workspace is an optimization problem, where parameters for the kinematic structure of the system are selected in such a way that a specific cost function is optimized for an optimal surgical system. The cost function depends on which aspect of the system should be improved. The patient-specific adaptation of the kinematic structure to the workspace is already applied in the field of continuum robots, which are often used in surgical fields with strong anatomical workspace limits. Four target criteria for system optimization are identified: observance of anatomical workspace limits [4], [5], [6], minimization of the geometric dimensions [7], [8], maximization of the size of (partial) workspaces [9], [10], and maximization of manipulability [11], [12], [13].

The kinematic structure of single incision laparoscopic systems is currently adapted once during the design process for a large number of patients and indications. These systems are not optimized for a specific patient with a specific indication, resulting in a larger workspace than needed and in less accuracy of the system because of the longer arms. Optimized systems could be created by adapting single incision laparoscopic systems to a specific patient. The design and construction process, which has to be highly automated to reduce personnel costs, is crucial.

A. Previous Work

Our long-term goal is the customization of surgical systems for endoscopy and laparoscopy to create optimized systems for a specific indication, procedure, patient, and surgeon by using an automated design and construction process and 3D printing for manufacturing [14]. The concept is that the surgical system should be modular and adaptive in regard to the structure, the control mode, and the integration of instrumentation and additional features. The structure should be composed of a set of standard elements and customizable elements that can be combined and adapted according to the input parameters. A mechanical or electronic control unit should be used. Different types of standard instruments and endoscopes should be integrated. The system should

*The authors would like to thank the Deutsche Forschungsgemeinschaft (DFG) for supporting the project LU 604/27-2.

Sandra V. Brecht, Johannes S. A. Voegerl and Tim C. Lueth are with the Department of Mechanical Engineering, Institute of Micro Technology and Medical Device Technology (MiMed) of the Technical University of Munich, Munich, Germany (corresponding author: phone: +49-89-289-15189; fax: +49 89 289-15192; e-mail: sandra.brecht@tum.de).

be extendable and adaptable for a wide range of minimally invasive applications.

In our previous work, we built endoscopic and laparoscopic manipulator systems that consist of an overtube structure for flexible standard instruments with actuatable arms and a flexible or rigid shaft and control units for controlling the arms via Bowden cables. The flexible instruments can be moved axially in the overtube structure. The arms are monolithically designed and consist of three sections for opening, moving up and down, and moving the arms left and right. Each section consists of several segments connected by flexure hinges. The systems are modular and therefore use as many standard elements as possible, e.g., for connectors or parts of the control units. To be able to adapt the system to the instrumentation used and the needed arm lengths and deflection angles, we used a parameterized design implemented with CAD software. For the endoscopic version, the first steps for an iterative adaption to the workspace were achieved [15], [16].

B. Novel Approach

We developed an automated design and construction process for a Single Incision Laparoscopic System that is adapted to the required workspace for a specific operation in a specific patient. The process also takes into account the surgeon's preferences regarding the instruments and endoscope used as well as the patient's anatomy. The boundary conditions of the 3D printing process are automatically considered. The process consists of five main steps, which are shown in Figure 1 and described in detail in Section II. The design and construction process is implemented completely in MATLAB (MathWorks, Inc., Natick, Massachusetts, USA).

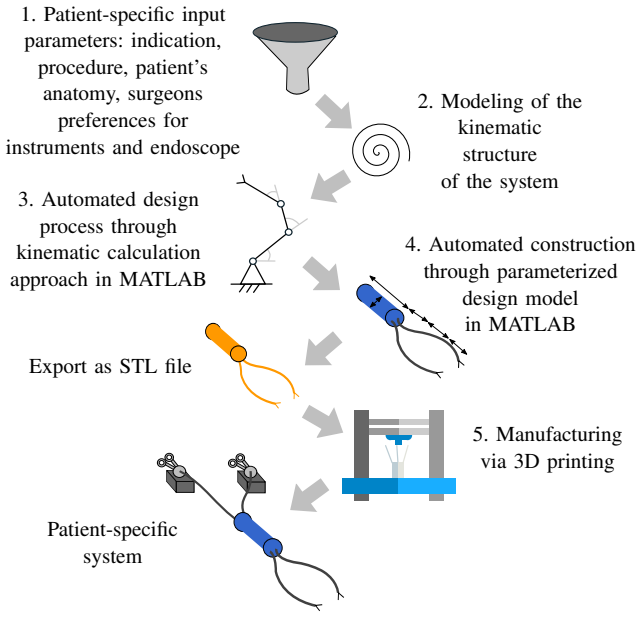

Fig. 1. Schematic illustration of the process for creating a patient-specific Single Incision Laparoscopic System.

1) Determination of input parameters: The first step is the determination of the input parameters of the surgeon for the laparoscopic procedure. They are the needed workspace and trocar access point (e.g., at the navel) based on the anatomical data of the patient as well as the instruments and endoscope used.

2) Modeling of the kinematic structure of the system: In the second step, the kinematic structure of the system is modeled in order to optimize the structure of the system. Certain parameters are then defined within the model, which can be changed during the design process.

3) Automated design of the system: In the next step, a target function is set up based on the kinematic structure, the model of the workspace, and the selected target criteria, which quantifies how well or poorly a system design meets the demanded requirements. Next, based on the objective function, and if necessary together with additional constraints, an optimization algorithm is used to determine the optimal values for the parameters determined in Step 2.

4) Automated construction of the system: Subsequently, the optimal values for the parameters are used as inputs for the automated construction process of the system that also automatically considers the manufacturing parameters of the 3D printing process.

5) Manufacturing: In the last step, the system is 3D printed.

With this novel approach for an automated design and construction of a patient-specific Single Incision Laparoscopic System, we believe that we can build systems that, in comparison with standard-sized systems, are better suited for a specific application concerning the combination of reachability, manipulability, and system size in the needed workspace.

II. MATERIALS AND METHODS

A. Determination of the Input Parameters

The surgeon determines the required instruments and endoscope as well as the trocar access point and the needed workspace in a graphical user interface. For the instruments and endoscope, we use the diameter and length as input parameters for the design process, which are stored in a database, so that the surgeon only has to select the appropriate instruments. The trocar position is determined by the surgeon relative to the position of the navel.

The input parameters for the needed workspace are described as an ellipsoid with its radii and its center position relative to the position of the navel. We use an ellipsoid since it fits the rounded shape of the workspaces of surgical systems and the rounded shapes of organs or tumors better than a cuboid. The workspace ellipsoid parameters can be determined according to the workspace needed for a specific surgical procedure, e.g., partial nephrectomy, or for specific tasks, e.g., suturing; or according to the patient's anatomy, e.g., organ or tumor size or available space in the abdomen. Preoperative imaging can be used for this. In future work, the automation of the process for determining the workspace based on preoperative image segmentation can be considered.

B. Modeling of the Kinematic Structure of the System

To be able to adapt the Single Incision Laparoscopic System described in [16] to the required workspace, the length of the shaft and the length and deflection angles of the three sections for opening, moving up and down, and turning the arms in and out are variable.

To simplify the design and construction of the manipulator arms, a combination of adaptable elements and standard elements, e.g., for the attachment of the Bowden cable, are used. Additionally, as few design parameters as possible should be used.

The kinematic structure consists of three sections with revolute joints for every section (yaw for the first q_1, pitch for the second q_2 and yaw for the third section q_3), one translation joint for the axial movement of the instrument q_4 and one revolute joint (roll) for the rotation of the effector q_5.

The revolute joints are implemented by multiple segments per section with flexure hinges. The flexure hinges are integrated with a maximum deflection angle of 10° to prevent failure. The required lengths as well as the deflection angles of the three sections can be adjusted via the number and height of the segments.

In summary, we have the following design parameters for the kinematic structure: Number of segments of the shaft with fixed length n_{Shaft}, number of the segments for the sections for opening n_{Out}, moving up and down n_{UpDown}, and turning the arms in and out $n_{LeftRight}$ with variable segment heights $h_{Segment}$. The kinematic structure of the shaft and one arm is shown in Figure 2.

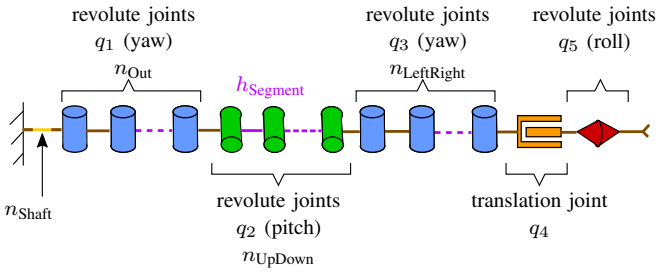

Fig. 2. Schematic illustration of the kinematic model of an arm with q_1 - q_5 and the design parameters n_{Shaft}, n_{Out}, n_{UpDown}, $n_{LeftRight}$ and $h_{Segment}$.

The workspace of the arms can be calculated using the forward kinematics. For this purpose, each flexure hinge is modeled in simplified form as a revolute joint. The forward kinematics are calculated using a matrix product of homogeneous transformation matrices, which are calculated in the form of function handles with q_1 - q_5.

C. Automated Design

For optimization of the five design parameters, a multi-objective optimization with the following target criteria is used in prioritized order: Maximization of the size of the workspace that can be reached with both arms (for maximum reachability of the needed workspace), minimization of the geometric dimensions (because of limited space conditions of Single Incision Laparoscopic Surgery, and better force transmission), maximization of the manipulability in the shared reachable domain (for maximum manipulability).

An overview of the design process is shown in Figure 3. The design process is described in the following.

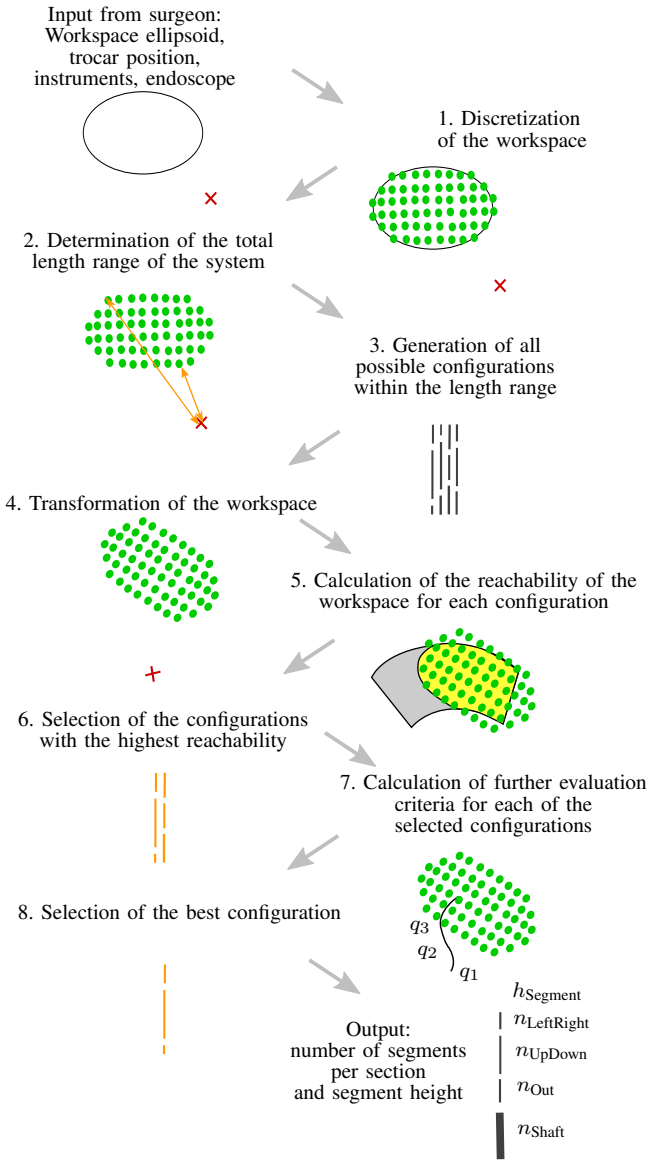

Fig. 3. Schematic illustration of the design process to determine the design parameters h_{Segment}, n_{Shaft}, n_{Out}, n_{UpDown}, and $n_{\text{LeftRight}}$ for an optimized system for a specific workspace.

Input: As input parameters, the trocar access point and the location of the center of the workspace ellipsoid and its radii are used. Additionally, the kinematic structure of the system and the values for the standard elements are stored.

1) Discretization of the workspace: In the first step of the process, the continuous workspaces are discretized with homogeneously distributed points to facilitate further calculations.

2) Determination of the total length range of the system: In the second step, the total length range of the

system is determined. For this purpose, the total length of the system is divided into the variable length and fixed length of the standard elements. The condition for all of the points in the working area to be reachable is that the minimum total length of the system must be at least equal to the distance from the trocar entry point to the furthest point of the workspace. If the total length of the system is shorter than the distance from the trocar entry point to the nearest point in the workspace, or much longer than the distance to the furthest away point in the workspace, no point in the workspace can be reached. The maximum length of the system is limited by the manufacturing process.

3) Generation of all possible configurations within the length range: Subsequently, all possible combinations of design parameters, hereinafter referred to as configurations, are generated within an area of the respective lower and upper limit values for each design parameter in steps of 1 mm for the length and steps of 1 for the number of segments, which results in several systems in the previously determined length range. For the number of segments for each section, the lower and upper limit values are defined by the minimum/maximum numbers to fulfill the function and minimum/maximum suitable deflection angles. The minimum height of the segments is determined according to the minimum necessary height to fulfill the function and the minimum bending radius of the arms because of the rigidity of the instrument. The maximum height is limited according to the maximum length of the system. Here, we use the following values for the lower and upper limits: $n_{Out} = [3; 4]$, $n_{UpDown} = [4; 9]$, $n_{LeftRight} = [1; 8]$, $h_{Segment} = [5; 15 \text{ mm}]$.

4) Transformation of the workspace: In the next step, the discretized workspace is transformed into a zero position to take into account the alignment of the system at the beginning of the surgery process.

5) Calculation of the reachability of the workspace: In the fifth step, in order to maximize the size of the workspace that can be reached with both arms, the reachability of the points of the workspace ellipsoid is calculated for each system configuration from Step 3. For this purpose, a point cloud of the achievable workspace of each arm is generated for each configuration using the forward kinematics. The workspace envelope is then generated from this point cloud using the *MATLAB alphaShape* function. The *MATLAB inShape* function is then used to test for each point of the transformed workspace ellipsoid, whether or not it lies within the workspace envelope of both arms. The reachability of the workspace ellipsoid is calculated for each configuration in scalar form as a percentage R_s of the reachable points of the total number of points in the workspace ellipsoid.

6) Selection of the configurations with the highest reachability: In Step 6, the configurations for which the highest values of reachability were determined in Step 5 (ideally with $R_s = 1$) are selected for further evaluation.

7) Calculation of further evaluation criteria: For the selected configurations with the highest reachability, further evaluation criteria are calculated. Here, we use the total lengths of the arms and the manipulability, which is a measure of the ability of the system to change its pose.

The lengths of the arms are calculated by summing the fixed and variable lengths.

The manipulability of every point in the workspace ellipsoid is calculated using the manipulability measure w with Equation 1 [17]. Subsequently, the mean manipulability m is calculated.

$$w = \sqrt{det(J_w(q) \cdot J_w^T(q))} \tag{1}$$

For the calculation of the manipulability measure w, the Jacobian matrix J_w of the system is required. Furthermore, $q = [q_1 - q_5]$ are necessary to reach the points of the workspace ellipsoid, since the Jacobian matrix depends on q. To determine q, the inverse kinematics of the respective configuration must be calculated. The inverse kinematics was not calculated analytically by inverting the equations of the forward kinematics, because the equations of the forward kinematics were too complex to be solved reliably and quickly. To determine q, the inverse kinematics is defined as an optimization problem that is solved with an optimization algorithm. The squared distance between the reachable points of the workspace ellipsoid of Step 5 and the end effector position defined as a function of q is chosen as the objective function. The *particleswarm* optimization algorithm of the *MATLAB Global Optimization Toolbox* is used with the respective upper and lower joint limits and four variables. The rotation of the effector q_5 is not taken into account since it does not influence the position of the end effector.

8) Selection of the best configuration: In order to be able to compare the configurations, scores are calculated for the other evaluation criteria using Equation 2 for the length score s_l and Equation 3 for the manipulability score s_m. The maximum and minimum values are the highest and lowest values calculated across all configurations. The lengths of the arms should be as short as possible to minimize the geometrical dimensions, and manipulability should be as high as possible.

$$s_l = \frac{l_{max} - l}{l_{max} - l_{min}} \tag{2}$$

$$s_m = \frac{m - m_{min}}{m_{max} - m_{min}} \tag{3}$$

To select the best configuration, a weighted sum of the individual scores of the other evaluation criteria is calculated with Equation 4 to address the aforementioned prioritized order of the target criteria.

$$s_{best} = \frac{2}{3} s_l + \frac{1}{3} s_m \tag{4}$$

Output: Lastly, the design parameters of the best configuration is the output of the design process, which is subsequently used for the construction process.

D. Automated Construction

The automated construction is done with the SG-Library toolbox, which allows the creation of surface models of geometrical bodies with MATLAB. In the SG library, solids are constructed with a surface model consisting of triangles, which is defined using a Vertex List (VL) and a Facet List (FL). The FL defines which three points from the VL form a triangle and in which direction its normal vector points. A body is stored as Solid Geometry (SG), which combines the aforementioned VL and FL in one data type. At the end of the construction process, the SGs created with the SG library can be exported into the Standard Triangulation/Tesselation Language (STL) format [18].

The system is separated in the connector to the control unit with shaft and the shaft with arms parts (Figure 4). The shaft with arms part is divided into the sections shaft, out, up-down, left-right, and umbrella.

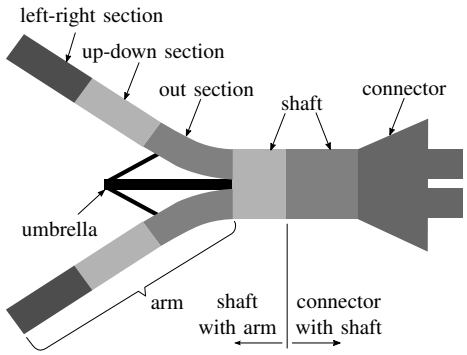

Fig. 4. Schematic illustration of the structure of the system consisting of a connector to the control unit with shaft, a shaft with arms consisting of the left-right section, up-down section and out section, and an umbrella part.

All the important variables for the construction are saved in a structure array, which is initialized with the input parameters of the surgeon for the instrumentation used and the results of the design process at the beginning of the construction process. In the structure array, all minimum and maximum values are stored, including error checks, boundary conditions for the 3D printing process, and standard values. Additionally, all parameterized dimensions for the variable parts are calculated, sometimes for different cases of input parameter combinations.

The shaft profile is the basis of the construction (Figure 5). The diameter of the shaft d_{shaft} and the instrument position circle d_{ipc} are calculated on the basis of the instrument diameter $d_{\text{instrument}}$, the endoscope diameter $d_{\text{endoscope}}$, and the spacing s according to Equations 5 and 6.

$$d_{\text{shaft}} = d_{\text{endoscope}} + 2 \cdot d_{\text{instrument}} + 4 \cdot s \tag{5}$$

$$d_{\text{ipc}} = d_{\text{endoscope}} + d_{\text{instrument}} + 2 \cdot s \tag{6}$$

The spacing s necessary for the calculation of the shaft diameter is determined depending on the instrument diameter $d_{\text{instrument}}$ and endoscope diameter $d_{\text{endoscope}}$ in such a way that a balanced profile is created to which the arm profile can be well connected. This good connection is achieved if Equation 7 applies, i.e., the geometry of the shaft is dominated by the inner part of the profile.

$$d_{\text{endoscope}} + 2 \cdot s \geq d_{\text{instrument}} \tag{7}$$

The arm profile forms the basis of the manipulator arms. The arm profile has a kidney shape and is shown in Figure 5. The arm profile is fitted into the shaft profile in such a way that on the one hand, the outer edge of the shaft profile and the endoscope channel are not exceeded, and on the other hand the available space within the shaft profile is used as fully as possible. The channels for the Bowden cables are positioned in such a way that they are symmetrically arranged at the greatest possible distance from the reference axis while maintaining the minimum distance to neighboring geometries.

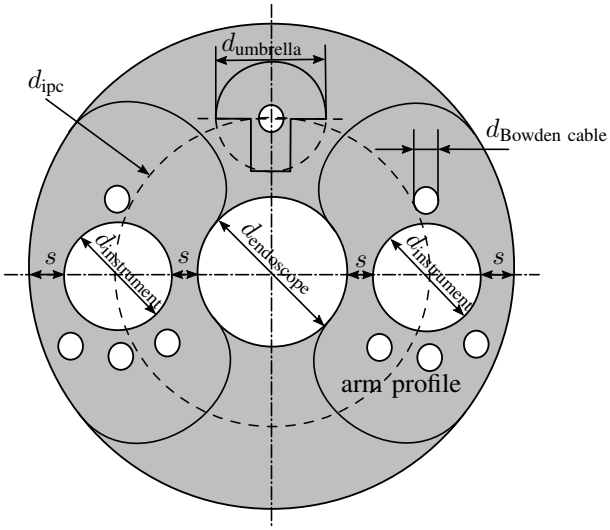

Fig. 5. Schematic illustration of the shaft profile and the arm profile with the shaft diameter d_{shaft}, the instrument position circle d_{ipc}, the instrument diameter $d_{\text{instrument}}$, the endoscope diameter $d_{\text{endoscope}}$, the diameter of the umbrella d_{umbrella}, the diameter of the Bowden cable channels $d_{\text{Bowden cable}}$ and the spacings s.

The individual sections of the system are divided into subsections, which can be assembled according to the modular design principle. An example is shown in Figure 6. Every section is constructed independently and all sections are subsequently put together.

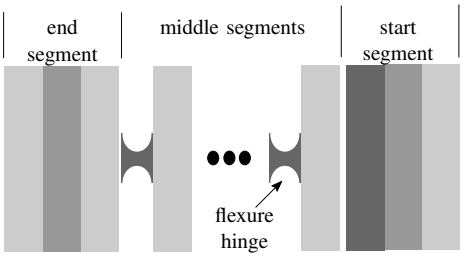

Fig. 6. Schematic illustration of the structure of the LeftRight section.

An example of the shaft with arms part exported into the STL format is shown in Figure 7. Lastly, the system

is manufactured using a validated selective laser sintering process with the EOS Formiga P100 (EOS GmbH, Krailing, Germany) using biocompatible PA 2200 powder (EOS GmbH, Krailing, Germany) and Bowden cables are inserted. An example of the system with instruments inserted is shown in Figure 8.

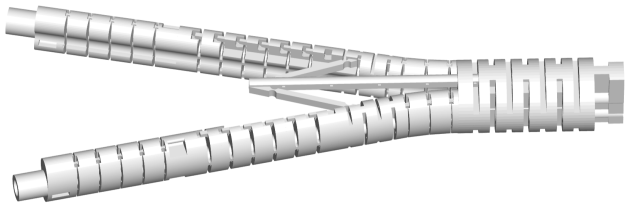

Fig. 7. Example of the shaft with arms part exported into the STL format.

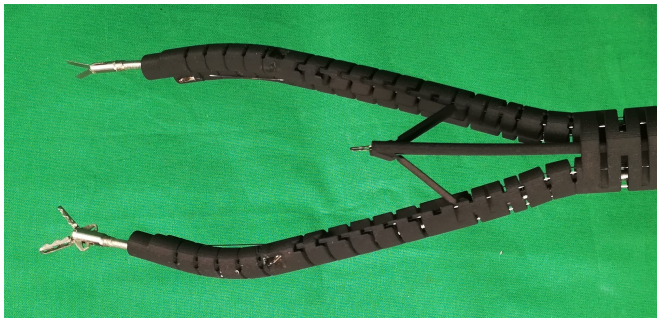

Fig. 8. Example of the manufactured system of Figure 7 with instruments inserted.

III. PRELIMINARY TESTS

To evaluate the need for customized systems, several systems were designed and tested in different workspaces regarding the combination of reachability, manipulability, and system size.

All systems were designed with an instrument channel diameter of 5.6 mm and an endoscope channel diameter of 6.5 mm. Three standard size systems S, M, and L were designed with $n_{shaft} = 2$, $n_{Out} = 4$, $n_{UpDown} = 6$, $n_{LeftRight} = 4$ and $h_{Segment} = 5$ mm for a minimum (standard S), $h_{Segment} = 7.5$ mm for a medium (standard M, similar to the kinematic structure of the Single Incision Laparoscopic System described in [16]) and $h_{Segment} = 10$ mm for a maximum (standard L) size. The maximum instrument translation is set to 30 mm for the SPIDER instruments (TransEnterix, Morrisville, NC, USA) used here. For each of these systems, the workspaces of both arms were calculated with the forward kinematics. In the area that can be reached with both arms, the maximum ellipsoid was created (here: workspace ellipsoid S, M, and L) that fits in this area. In addition to all standard size systems, customized systems (patient-specific S, M and L) with the calculated workspace ellipsoids as input parameters were designed using the automated design process described in Subsection II-C. Additionally, two intermediate customized systems (patient-specific SM, patient-specific ML) were designed with workspace ellipsoids with averaged radii and positions between the standard size workspace ellipsoids.

For every useful combination of workspace ellipsoid and system size, the length score (Equation 2), manipulability score (Equation 3), reachability score (Equation 8), and a weighted total score (Equation 9) were subsequently calculated with the minimum and maximum values from the respective systems tested in one workspace ellipsoid.

$$s_r = \frac{r - r_{min}}{r_{max} - r_{min}} \tag{8}$$

$$s_{total} = \frac{1}{2}s_r + \frac{1}{2}\left(\frac{2}{3}s_l + \frac{1}{3}s_m\right) \tag{9}$$

In order to be able to test the systems in the workspaces, the respective system was axially shifted in such a way that the workspace ellipsoid can be reached in the best possible way, but with the system pushed into the trocar just enough that the arms can still move.

IV. RESULTS

An overview of the total scores of the different systems tested in the different workspaces is shown in Table I. Here, systems with longer arm lengths tend to show better reachability and manipulability in smaller workspace ellipsoids than vice versa. System standard L cannot reach workspace ellipsoid S because its arms are too long.

TABLE I
TOTAL SCORES OF THE SYSTEM IN WORKSPACE ELLIPSOID TESTS

	Workspace				
System	S	SM	M	ML	L
standard S	0.94	0.33	0.32	-	0.33
patient-specific S	0.94	-	-	-	-
patient-specific SM	-	1.00	-	-	-
standard M	0.83	0.54	0.74	0.16	0.56
patient-specific M	-	-	0.83	-	-
patient-specific ML	-	-	-	0.83	-
standard L	0,00	-	0.67	0.67	0.59
patient-specific L	-	-	-	-	0.77

A. Standard size vs. S, M, L size

The comparison of the total scores in Table I shows that the total scores of system standard M in the workspace ellipsoids S and L are lower than the ones of systems standard S and standard L. For every workspace ellipsoid S, M, L, its corresponding standard system S, M, L has the best result.

B. S, M, L size vs. customized size

For the intermediate SM workspace ellipsoid, the total scores of the systems standard S and standard M tested in this workspace are lower than the total score of the system patient-specific SM, which was specifically designed for this workspace. The same applies to the systems standard M and standard L tested in the workspace ellipsoid ML. For all other patient-specific systems, the total scores are higher than the total scores of the respective standard systems in the

corresponding workspace, despite system standard S, where the system patient-specific S has the same configuration as system standard S.

V. DISCUSSION AND CONCLUSION

The first comparison between one standard size and several standard sizes shows that more standard sizes are better suited for all workspace ellipsoids. Systems with longer arm lengths tend to have better reachability and manipulability, but can only reach workspace ellipsoids at a certain distance from the trocar because their arms are much longer and therefore require a larger range of motion. Additionally, longer arms have higher flexibility and therefore less precision. Patient-specific systems are better suited for specific applications in terms of the combination of reachability, manipulability, and arm length in the required workspace than standard systems of different sizes or one simple standard size system. Further evaluation of patient-specific systems in comparison to standard systems in different sizes or one standard size system should be conducted, especially in the clinical environment and according to costs. Additionally, all further steps to complete the whole process, from the surgeon's input of the input parameters to the sterilized product in the operation room, should be implemented. In this context, the automation of the process for the determination of the workspace based on preoperative image segmentation can be integrated in order to also automate the input process. Moreover, to reduce the calculation time for the design process, a database with the results of reachability and manipulability in a large point cloud for often-used instrumentations and all configurations could be implemented, so that one would only have to select the relevant points of the desired workspace from the point cloud in order to calculate the total scores of the suitable configurations.

In summary, we have developed an automated design and construction process for a Single Incision Laparoscopic System that is adapted to the required workspace for a specific surgery in a specific patient. The process also takes into account the surgeon's preferences regarding the instruments and endoscope used, the patient's anatomy, and the manufacturing parameters of the 3D printing process. The whole design and construction process is implemented in one software program (MATLAB (MathWorks, Inc., Natick, Massachusetts, USA)). The few input parameters for instrumentation, workspace, and the trocar entry point can be set via a graphical user interface; the automated design process calculates the best configuration for the kinematic structure in regard to reachability, manipulability, and arm lengths and the automated construction process creates an STL-file, which can then be manufactured via selective laser sintering. We were able to demonstrate that the entire process from inputting parameters to manufacturing a patient-specific system is feasible.

ACKNOWLEDGMENT

The authors would like to thank the Deutsche Forschungsgemeinschaft (DFG) for supporting the project LU 604/27-2.

REFERENCES

[1] C.-Y. Liaw and M. Guvendiren, "Current and emerging applications of 3D printing in medicine," *Biofabrication*, vol. 9, no. 2, p. 024102, 2017.

[2] J. Borchard, J. Kotlarski, and T. Ortmaier, "Workspace comparison of cooperating instruments in laparo-endoscopic single-site surgery," in *2013 IEEE/ASME International Conference on Advanced Intelligent Mechatronics*, July 2013, pp. 1241–1248.

[3] B. Cheon, E. Gezgin, D. K. Ji, M. Tomikawa, M. Hashizume, H.-J. Kim, and J. Hong, "A single port laparoscopic surgery robot with high force transmission and a large workspace," *Surgical endoscopy*, vol. 28, no. 9, pp. 2719–2729, 2014.

[4] L. G. Torres, R. J. Webster, and R. Alterovitz, "Task-oriented design of concentric tube robots using mechanics-based models," in *2012 IEEE/RSJ International Conference on Intelligent Robots and Systems*. IEEE, 2012, pp. 4449–4455.

[5] T. K. Morimoto, J. J. Cerrolaza, M. H. Hsieh, K. Cleary, A. M. Okamura, and M. G. Linguraru, "Design of patient-specific concentric tube robots using path planning from 3-D ultrasound," in *2017 39th Annual International Conference of the IEEE Engineering in Medicine and Biology Society (EMBC)*, July 2017, pp. 165–168.

[6] T. Anor, J. R. Madsen, and P. Dupont, "Algorithms for design of continuum robots using the concentric tubes approach: A neurosurgical example," in *2011 IEEE International Conference on Robotics and Automation*, May 2011, pp. 667–673.

[7] C. Bedell, J. Lock, A. Gosline, and P. E. Dupont, "Design optimization of concentric tube robots based on task and anatomical constraints," in *2011 IEEE International Conference on Robotics and Automation*, May 2011, pp. 398–403.

[8] C. Bergeles, A. H. Gosline, N. V. Vasilyev, P. J. Codd, P. J. Del Nido, and P. E. Dupont, "Concentric tube robot design and optimization based on task and anatomical constraints," *IEEE Transactions on Robotics*, vol. 31, no. 1, pp. 67–84, 2015.

[9] J. Burgner, H. B. Gilbert, and R. J. Webster, "On the computational design of concentric tube robots: Incorporating volume-based objectives," in *2013 IEEE International Conference on Robotics and Automation*, May 2013, pp. 1193–1198.

[10] C. Baykal, L. G. Torres, and R. Alterovitz, "Optimizing design parameters for sets of concentric tube robots using sampling-based motion planning," in *2015 IEEE/RSJ International Conference on Intelligent Robots and Systems (IROS)*, Sep. 2015, pp. 4381–4387.

[11] A. B. Prasai, A. Jaiprakash, A. K. Pandey, R. Crawford, J. Roberts, and L. Wu, "Design and fabrication of a disposable micro end effector for concentric tube robots," in *2016 14th International Conference on Control, Automation, Robotics and Vision (ICARCV)*. IEEE, 2016, pp. 1–6.

[12] L. Wu, R. Crawford, and J. Roberts, "Dexterity analysis of three 6-DOF continuum robots combining concentric tube mechanisms and cable-driven mechanisms," *IEEE Robotics and Automation Letters*, vol. 2, no. 2, pp. 514–521, 2017.

[13] A. Razjigaev, A. K. Pandey, J. Roberts, and L. Wu, "Optimal dexterity for a snake-like surgical manipulator using patient-specific task-space constraints in a computational design algorithm." [Online]. Available: http://arxiv.org/pdf/1903.02217v1

[14] Y. S. Krieger, D. B. Roppenecker, J.-U. Stolzenburg, and T. C. Lueth, "First step towards an automated designed multi-arm snake-like robot for minimally invasive surgery," in *2016 6th IEEE International Conference on Biomedical Robotics and Biomechatronics (BioRob)*, June 2016, pp. 407–412.

[15] Y. S. Krieger, D. B. Roppenecker, I. Kuru, and T. C. Lueth, "Multi-arm snake-like robot," in *2017 IEEE International Conference on Robotics and Automation (ICRA)*, May 2017, pp. 2490–2495.

[16] S. V. Brecht, M. Stock, J.-U. Stolzenburg, and T. C. Lueth, "3D printed single incision laparoscopic manipulator system adapted to the required forces in laparoscopic surgery," in *2019 IEEE/RSJ International Conference on Intelligent Robots and Systems (IROS)*, Nov 2019, pp. 6296–6301.

[17] J. J. Craig, *Introduction to robotics: Mechanics and control*, 3rd ed. Upper Saddle River, N.J: Pearson/Prentice Hall, 2005.

[18] T. C. Lueth, "SG-Lib-Matlab-Toolbox," 2020. [Online]. Available: https://www.github.com/timlueth/SG-Lib-Matlab-Toolbox